Friction **11**(3): 441–459 (2023)
https://doi.org/10.1007/s40544-022-0619-4
ISSN 2223-7690
CN 10-1237/TH
RESEARCH ARTICLE

Synthesis of N-doped carbon quantum dots as lubricant additive to enhance the tribological behavior of MoS_2 nanofluid

Jiaqi HE[1,2], Jianlin SUN[1,*], Junho CHOI[2], Chenglong WANG[1], Daoxin SU[1]

[1] *School of Materials Science and Engineering, University of Science and Technology Beijing, Beijing 100083, China*

[2] *Department of Mechanical Engineering, The University of Tokyo, Tokyo 113-8656, Japan*

Received: 12 November 2021 / Revised: 24 December 2021 / Accepted: 08 March 2022

Abstract: In this study, a novel lubricant additive nitrogen-doped carbon quantum dot (N-CQD) nanoparticle was prepared by the solvothermal method. The synthesized spherical N-CQD nanoparticles in the diameter of about 10 nm had a graphene oxide (GO)-like structure with various oxygen (O)- and nitrogen (N)-containing functional groups. Then N-CQDs were added to MoS_2 nanofluid, and the tribological properties for steel/steel friction pairs were evaluated using a pin-on-disk tribometer. Non-equilibrium molecular dynamics (NEMD) simulations for the friction system with MoS_2 or MoS_2 + N-CQD nanoparticles were also conducted. The results showed that friction processes with MoS_2 + N-CQD nanofluids were under the mixed lubrication regime. And MoS_2 nanofluid containing 0.4 wt% N-CQDs could achieve 30.4% and 31.0% reduction in the friction coefficient and wear rate, respectively, compared to those without N-CQDs. By analyzing the worn surface topography and chemical compositions, the excellent lubrication performance resulted from the formation of tribochemistry-induced tribofilm. The average thickness of tribofilm was about 13.9 nm, and it was composed of amorphous substances, ultrafine crystalline nanoparticles, and self-lubricating $FeSO_4$/$Fe_2(SO_4)_3$. NEMD simulation results indicated the interaction between S atoms in MoS_2 as well as these O- and N-containing functional groups in N-CQDs with steel surfaces enhanced the stability and strength of tribofilm. Thereby the metal surface was further protected from friction and wear.

Keywords: carbon-based quantum dots (CQDs); lubricant; nanofluid; molecular dynamics (MD); tribofilm

1 Introduction

Recently, friction and wear have become one of the major factors causing material and energy consumption. Lowering friction coefficient and wear rate are of great importance for improving the efficiency of metal-working processes [1] and prolonging the service life of mechanical equipment [2]. The adoption of appropriate lubricants is a powerful and convenient means to solve the issues. With the advancement of nanotechnology, nanoparticles with unique physicochemical properties and excellent tribological behaviors become the research hotspot, and they have a broad application prospect as solid lubricants or fluid-lubricant additives [3, 4]. However, due to their high specific surface area and surface energy, nanoparticles are easy to agglomerate in fluids; thereby the development of stable nano-lubricants with excellent lubrication performance is an eternal topic nowadays.

As promising zero-dimension nanomaterials, quantum dots (QDs) with the diameter of 1–10 nm, such as metal-based quantum dots (MQDs) [5], silicon-based quantum dots (SQDs) [6], and carbon-based quantum dots (CQDs) [7] have been widely applied in the field of photovoltaic device, biomedicine, and

* Corresponding author: Jianlin SUN, E-mail: sjl@ustb.edu.cn

renewable energy in the past decades. Among these kinds of QDs, the heavy metal elements in MQDs are potentially harmful to the environment, and the preparation of SQDs is still complex and costly. In contrast, CQDs composed of carbon (C) cores and surface groups were highlighted in the field of lubrication due to their low toxicity and environmental friendliness [8]. In the investigation of Tang et al. [9], CQDs were synthesized and applied in water-based lubricants as an additive for amorphous coatings. The results indicated that the introduction of CQDs into lubricant at a concentration of 0.1 wt% could reduce friction and wear by about 33% and 80%. Xiao et al. [10] prepared S-doped CQDs using hydrothermal method as water-based lubricant additive for Si_3N_4–steel and Si_3N_4–Si_3N_4 friction pairs. These nanoparticles improved the formation of tribofilm to protect the surfaces from friction and wear. More importantly, the related studies also reveal that the structure, composition, and size of CQDs can be designed and controlled artificially [11, 12]. Hence, surface functionalization and elemental doping of CQDs can be achieved, which can further improve the dispersion stability and chemical activity. Then their tribological behaviors in lubricants can be enhanced due to the tribochemical reactions between these functional groups/doped atoms and the friction surface. Tu et al. [13] compared the lubrication performance of plain CQDs and Ni-doped CQDs (Ni-CQDs). The lower friction coefficient and wear rate of PEG200 containing Ni-CQDs were ascribed to the tribofilm formed by doped Ni atoms and other groups. Sarno et al. [14] prepared CQD–poly(methyl methacrylate) nanocomposite for tribological application. It was found that the ball-bearing effect and continuous deposition of CQDs at the metal surface decreased the friction significantly. Mou et al. [15] designed a series of functionalized CQDs with various anionic groups, such as hexafluorophosphate (PF_6^-), bis-(trifluoromethane)–sulfonimide (NTf_2^-), and oleate (OL^-). The results showed that OL^--modified CQDs had the best load-capacity and lubricating performance, which was attributed to the formation of organic–inorganic hybrid adsorption film by the interaction of neutralizing carboxylic groups (COO^-) with metal surfaces. Therefore, surface functionalization and elemental doping of CQDs, as well as their application in the field of lubrication, are important development directions in the future. The influence of these factors on lubrication mechanism still needs to be thoroughly discovered. And as a kind of active atom, nitrogen (N) atom has strong affinity with metal through hydrogen bond, van der Waals attraction, etc. Hence, we considered preparing nitrogen-doped carbon quantum dots (N-CQDs) as lubricant additive.

It is well known that the co-use of different kinds of nanoparticles can achieve better tribological properties due to the synergistic lubrication effect, such as MoS_2/Al_2O_3 [16], Cu/graphene [17], graphene oxide (GO)/TiO_2 [18], and Fe_3O_4/MoS_2 [19] hybrid nanofluids. Besides, although QDs usually possess outstanding lubrication performance compared with traditional nanoparticles, the relatively higher cost and lower efficiency of the synthesis process limit their popularization and wide application to some extent [8, 20]. Furthermore, as a kind of widely-used solid lubricant for a long time, MoS_2 nanoparticle is lately applied more frequently as lubricant additive. Due to the lamellar structure and excellent film-forming ability, MoS_2 nanoparticle exhibits favorable anti-friction and anti-wear properties. Hence, we added N-CQDs to MoS_2 water-based nanofluid as lubricant. On one hand, the tribological behavior of MoS_2 nanofluid can be further regulated. On the other hand, it can achieve a balance between environmental friendliness and lower expenditure.

Based on the previous studies by relevant scholars, the lubrication mechanisms of nanoparticles are proposed and summarized into the polishing effect [21], mending effect [22], rolling effect [23], interlayer sliding effect [16, 24], and protective film [3, 25]. However, these viewpoints are mainly inferred from experimental results. Direct evidence and theoretical support are still lacking, and there is also some doubt about the actual existence of these effects [26]. Fortunately, the non-equilibrium molecular dynamics (NEMD) method has become a powerful and effective tool to address the above issue. Through NEMD simulation, the friction and wear processes for systems with lubricants can be predicted or reproduced. By capturing and analyzing the motion, force, and other physical quantities of atoms in the simulation system,

the essence of lubrication mechanisms will be revealed from the micro-level. NEMD method has been successfully employed in lubricant research such as the traditional lubricating oil [27], organic additives [28], and nanofluid [29]. Therefore, NEMD simulation is suitable to study the behavior of N-CQD nanoparticles in MoS_2 nanofluid.

In this study, N-CQD nanoparticles were synthesized by a simple solvothermal method using dopamine as the C and N source firstly. The prepared N-CQD nanoparticles were added in MoS_2 nanofluid as additive. Then, the tribological properties of nanofluid-containing N-CQDs were studied using a pin-on-disk tribometer. The topography and chemical compositions of the worn surface were analyzed, and the tribofilm generated at the friction interface was also characterized to reveal the lubrication mechanism. Finally, NEMD simulations were conducted to capture the diffusion of atoms during friction processes, thus discovering the function of N-CQDs on the formation of tribofilm from the atomic scale.

2 Experimental

2.1 Materials and reagents

MoS_2 nanoparticles (> 99%, 2H-phase, 100 nm) were gained from Macklin Biochemical, Co., Ltd., Shanghai, China. Dopamine hydrochloride (> 98%), sodium hexametaphosphate (SHMP, CP), and sodium dodecylbenzene sulfonate (SDBS, AR) were obtained from Aladdin Reagent Co., Ltd., Shanghai, China. Glycerol (> 98%), ethanol (AR), carboxymethylcellulose (CMC, M_W = 700,000 Da), NaOH, and HNO_3 were provided by Sinopharm Chemical Reagent Co., Ltd., Beijing, China. All materials and reagents were used as received without any further purification.

2.2 Preparation of N-CQDs and lubricants

N-CQD nanomaterial was synthesized using the solvothermal method, as shown in Fig. 1. Firstly, dopamine hydrochloride was added to the NaOH solution and stirred for 15 min to neutralize the hydrochloric acid in the reagent. Subsequently, excessive HNO_3 was added to the dopamine solution as the carbonizing agent and the mixture was stirred for 1 h. Afterwards, the solution was transferred to a Teflon-lined stainless-steel autoclave and maintained at 180 °C for 15 h to provide enough heat and time to ensure these ingredients react adequately. The products were filtered and rinsed by deionized water for several times. Then the fluid was dialyzed for 30 h at 25 °C in a dialysis bag (retained molecule weight of 2,000 g·mol^{-1}) to remove residual impurities. The remaining fluid was freeze-dried for 24 h in a

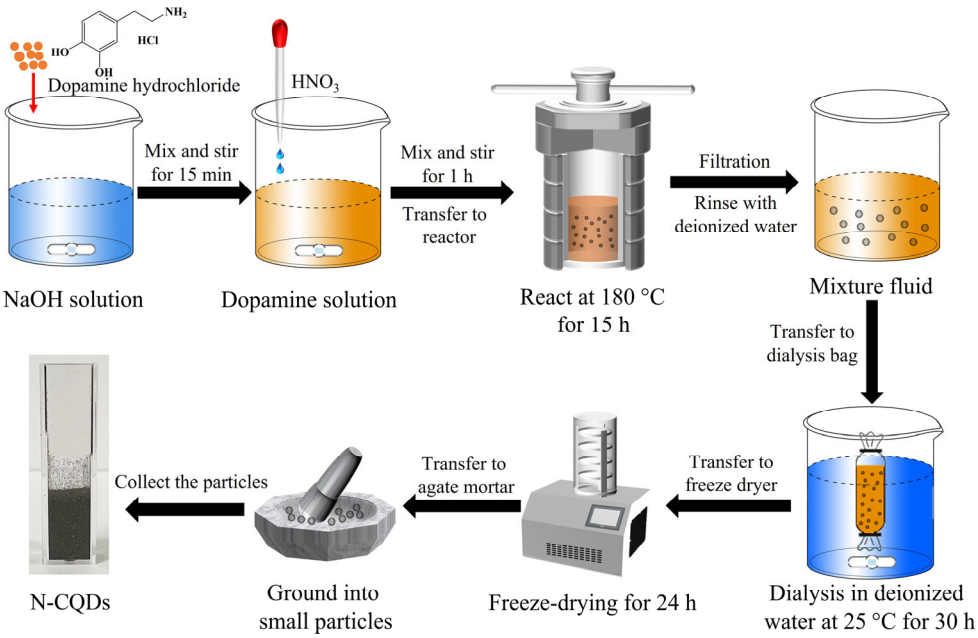

Fig. 1 Preparation process of N-CQDs.

freeze dryer (Scientz-10N, Scientz Co., Ltd., China) to gain N-CQD powders. Finally, the obtained powders were ground into small particles in an agate mortar.

MoS_2 nanofluid and hybrid nanofluid containing both MoS_2 and N-CQDs were prepared as lubricants. The preparation processes of these nanofluids were as follows. Firstly, glycerol and CMC were added to the deionized water successively under continuous stir at 60 °C. Then, SHMP and SDBS were added to the fluid as dispersant and surfactant, respectively. Finally, nanoparticles were added to the solution according to the corresponding concentration. After being stirred at 60 °C for 15 min and sonicated at 50 °C for 30 min, nanofluids with superior stability and homogeneity were obtained. The content of MoS_2 nanoparticles in each nanofluid was 0.5 wt%. And the concentrations of N-CQDs in the five groups of hybrid nanofluids were 0.1, 0.2, 0.3, 0.4, and 0.5 wt%, respectively. Besides, base fluid without nanoparticles was also prepared as the control group according to these steps, and other components in the base fluid were identical to the nanofluid.

To evaluate the dispersion stability, the photos of these nanofluids just-prepared and aging for 168 h were provided. And an ultraviolet–visible (UV–vis) spectrophotometer (UV-6100, Mapada, China) was employed to measure the variation of relative concentrations for different nanofluids. These results were presented in Fig. S1 in the Electronic Supplementary Material (ESM). After 168 h of storage, obvious sediments could be found in the bottom of the six groups of nanofluids. The color of MoS_2 nanofluid became lighter and its relative concentration was the lowest at every time, while the fading phenomenon of nanofluid-containing N-CQDs was not obvious. Therefore, N-CQDs exhibited excellent dispersion stability in the fluid. Although MoS_2 nanoparticles have agglomerated to some extent, the presented dispersion performance was enough for the study to investigate the lubrication performance of N-CQDs in nanofluids.

The shearing rheology curves for lubricants at different shearing rates γ were shown in Fig. 2. With the increase of γ from 1 to 30 s^{-1}, the dynamic viscosity η of all lubricants reduced obviously. Then η of the base fluid was basically constant. For these six groups of nanofluids, η rebounded at higher γ. η also increased with the rise of nanoparticle concentration. Therefore, the base fluid and nanofluids exhibited in this study were all non-Newtonian fluids with the shear thinning behavior. This characteristic was due to the addition of dispersants and other organic additives in the fluids. However, when γ was very high, the shear force would break down the interaction between nanoparticles and lead to the agglomeration, thus improving the apparent η [30].

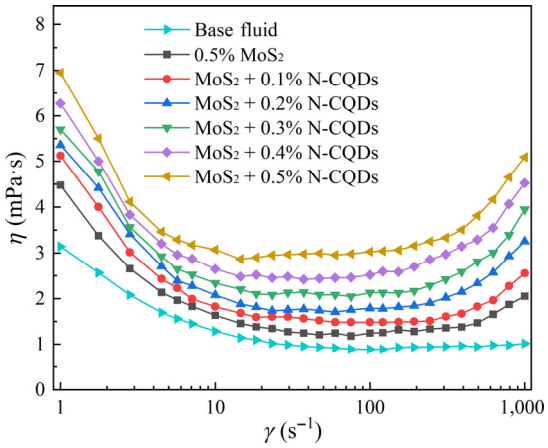

Fig. 2 Variation of η with γ for different lubricants.

2.3 Pin-on-disk tribological tests

The tribological behavior of different lubricants was investigated using a pin-on-disk tribometer (MM-W1A, Jinan Shijin Testing Machine Co., Ltd., China). As shown in Fig. 3, in the presence of lubricant, the steel pin was loaded and rotated against the fixed steel disk to achieve sliding friction for 3,600 s according to the standard ASTM G99-2017. The pin and disk were made of AISI 1045 steel, and the chemical compositions were presented in Table 1. The friction coefficient μ was measured once per second during tests, and the wear rate W_r of teel disk was also obtained by Eq. (1):

$$W_r = \Delta W/(\rho l N) \quad (1)$$

where ΔW is the wear loss weight of disk, ρ is the density of disk (7.85 g·cm^{-3}), l is the friction distance of friction pairs, and N is the test load. All tribological tests were conducted three times, and the wear rate values were also calculated three times to eliminate the occasionality of the results.

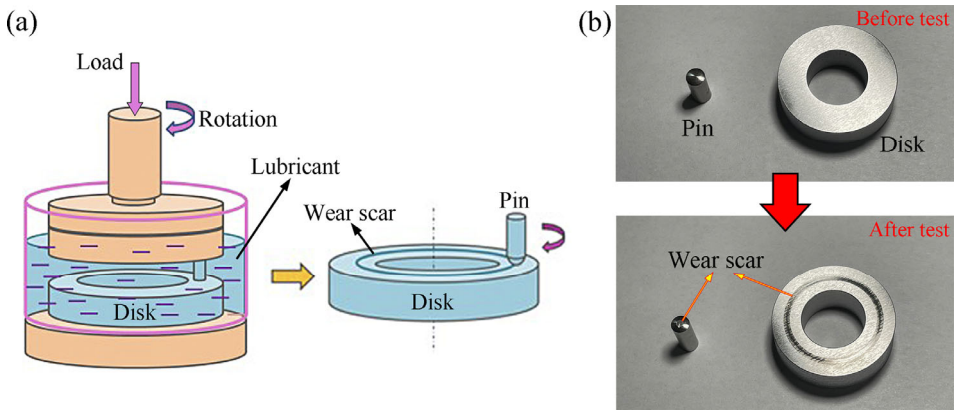

Fig. 3 (a) Schematic diagram of the pin-on-disk tribometer and (b) photos of the pin and disk before and after test.

Table 1 Chemical compositions of the steel pin and disk for tribological tests.

Element	C	Si	Mn	Cr	S	Fe
Content (wt%)	0.42	0.18	0.49	0.22	⩽ 0.03	Balance

2.4 Characterization methods

The microstructures and chemical compositions of N-CQDs were characterized using the transmission electron microscope (TEM; JEOL JEM-2010, Japan), X-ray photoelectron spectroscope (XPS; Kratos AXIS Ultra, Japan), Raman spectroscope (LabRAM, HR Evolution, America) with a 532 nm laser source, and Fourier transform infrared (FT-IR) spectroscope (Bruker Vertex 70, Germany). The worn surface of disk was analyzed by the laser scanning confocal microscope (LSCM; Olympus LEXTOLS 4100, Japan), scanning electron microscope (SEM; ZEISS Sigma 500, Germany) equipped with the energy dispersive spectrometer (EDS) and XPS. To gain the structure and composition of the tribofilm formed by nanofluids, TEM and EDS were employed, and the TEM sample was acquired via the focused ion beam (FIB) microscope (Helios Nanolab 600i, FEI, USA).

2.5 Molecular dynamics (MD) simulation

To further determine the lubrication mechanism of N-CQDs in nanofluid at the atomic scale, MD simulation was conducted to study the dynamic diffusion and distribution of atoms between friction pairs. As shown in Fig. 4, two simulation models containing MoS_2 nanoparticles (Fig. 4(a)) as well as both MoS_2 and N-CQDs (Fig. 4(b)) were built to simulate friction process under nanofluid lubrication. The focus of this study was on the behavior of nanoparticles, meanwhile, there are usually not enough liquid lubricants in the contact interface to prevent direct contact of friction pair surface in the boundary and mixed lubrication conditions [31]. Hence, no fluid molecules were included in these simulation models. These nanoparticles were placed between two iron

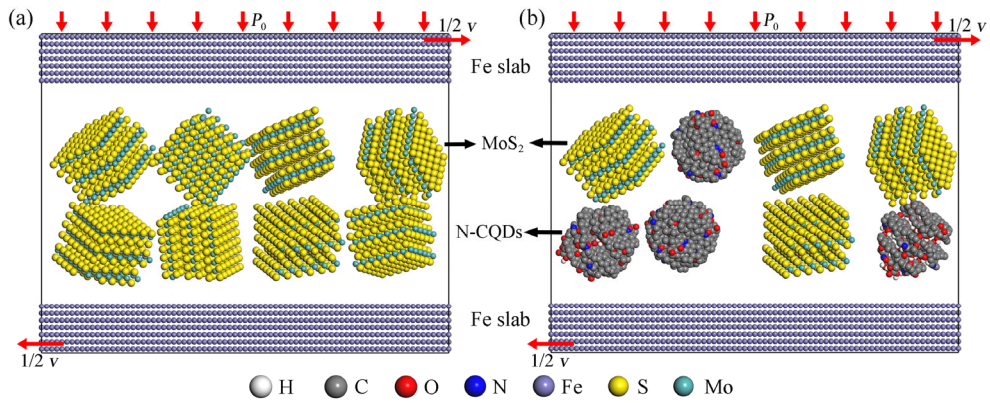

Fig. 4 (a) Schematic diagram of the pin-on-disk tribometer and (b) photos of the pin and disk before and after test.

slabs, and the dimension of the models was 114 Å × 40 Å × 90 Å. The interatomic interactions between metal atoms were modified by the embedded atom method (EAM) potential [32], and meanwhile, the van der Waals interactions between atoms were modified using the 12–6 Lennard–Jones potential [33].

After the above model setup stage, the dynamics simulation stage was performed. Firstly, the pressure P_0 = 100 MPa was applied along the z-direction to simulate the pressure during actual friction process. And the temperature was maintained at 298 K using the Nose–Hoover thermostat [34]. Then the models were relaxed adequately for 200 ps to reach the equilibrium state under the canonical (NVT) ensemble. Afterwards, the confined shear process was performed under the microcanonical (NVE) ensemble. The top and bottom Fe slabs were moved in the opposite direction along x-direction at the relative velocity v = 0.05 Å·ps^{-1} (5 m·s^{-1}) to simulate the sliding friction process. The sliding process lasted for 1,000 ps with a time step of 1 fs. The motion trajectory and velocity of atoms were recorded and exported every 10 ps.

3 Results and discussion

3.1 Characterization of N-CQD nanoparticles

The TEM, high-resolution transmission electron microscope (HRTEM), and corresponding fast Fourier transform (FFT) images of N-CQDs were shown in Fig. 5. It could be seen that the size of N-CQDs was approximately 10 nm in diameter, indicating that the synthesized nanoparticles were indeed QDs. From the HRTEM and FFT diffraction patterns, the interlayer distances of 0.179 and 0.211 nm in Fig. 5(b) were in accordance with the (102) and (100) planes of graphite, respectively (JCPDS card No. 75-1621), and the diffraction rings in Fig. 5(c) with the interlayer distances of 0.212 and 0.337 nm matched (100) and (002) planes, respectively. The result indicated that N-CQDs exhibited good crystallinity with a significant polycrystalline structure.

The chemical compositions of N-CQDs were further analyzed by the XPS, and the results were presented in Fig. 6. The following XPS analysis was referred to the National Institute of Standards and Technology (NIST) Standard Database 20 (Version 4.1). The wide-scan spectrum in Fig. 6(a) showed that N-CQDs were certainly composed of C, O, and N elements, which indicated that N-CQDs were doped by N atoms, and a certain number of oxygen (O)- and N-containing functional groups were attached to particles [35]. The peaks at 284.6, 286.0, 287.8, and 288.7 eV in C 1s spectrum (Fig. 6(b)) were related to C–C/C=C, C–N/C–OH, epoxy group (C–O–C), and carboxyl group (–COOH), respectively. Meanwhile, the O 1s peaks at 530.9 eV (C=O) and 532.6 eV (C–O) in Fig. 6(d) also proved the presence of C–O–C and –COOH in N-CQDs, respectively. The N 1s spectrum (Fig. 6(c)) was divided into three peaks at 397.7, 400.0, and 401.6 eV corresponded to pyridinic N, pyrrolic N, and quaternary N, respectively.

The Raman spectra of N-CQDs and reference graphene were shown in Fig. 7(a). Compared with the Raman spectrum of graphene, the presence of D-band at 1,340 cm^{-1}, D+G band at 2,909 cm^{-1}, and broadening of G-band at about 1,576 cm^{-1} for N-CQDs indicated the decrease in the size of the in-plane sp^2

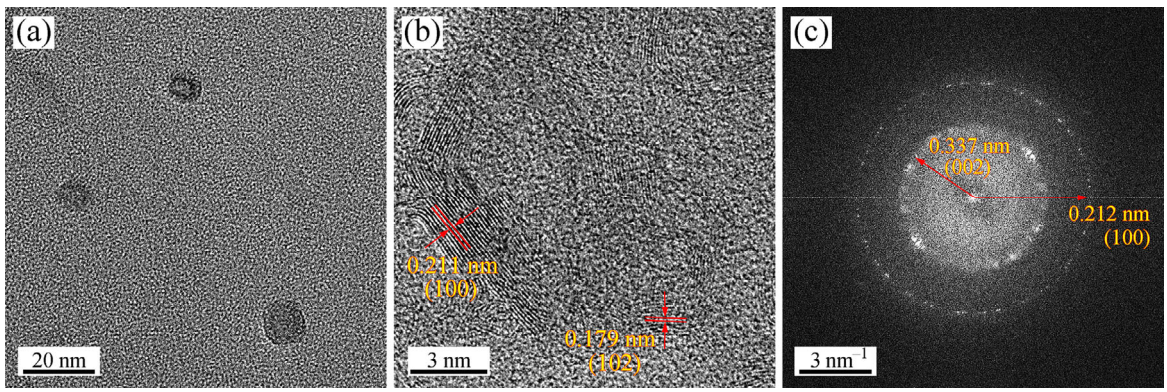

Fig. 5 (a) TEM, (b) HRTEM, and (c) FFT images of N-CQDs.

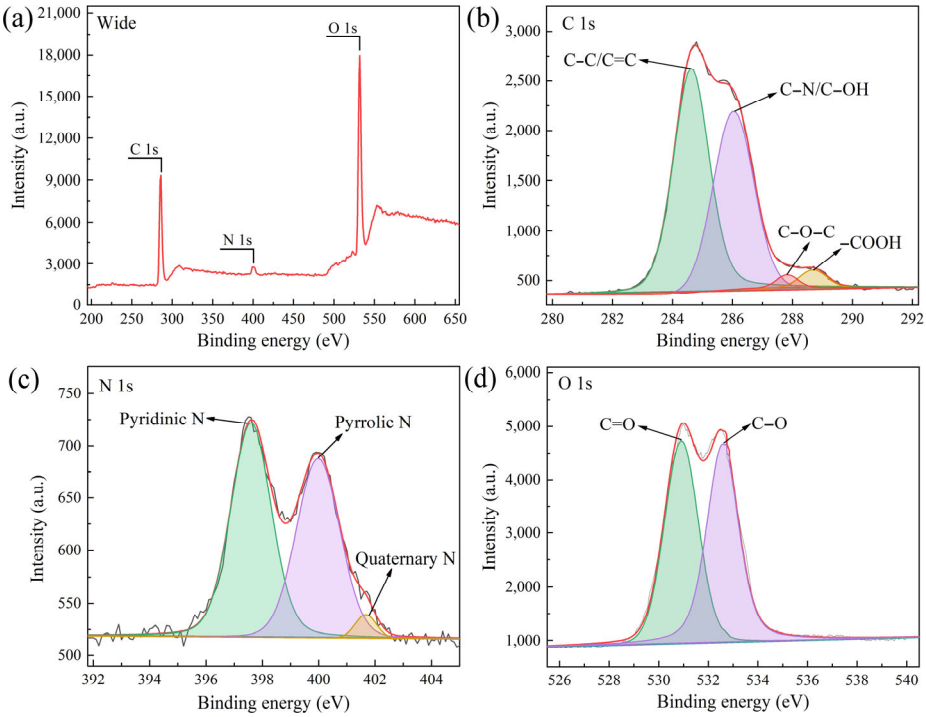

Fig. 6 XPS spectra of N-CQDs: (a) wide-scan, (b) C 1s, (c) N 1s, and (d) O 1s spectra.

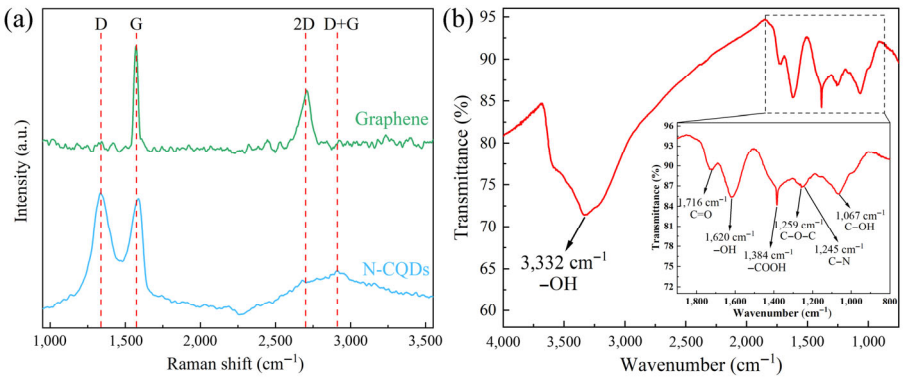

Fig. 7 (a) Raman and (b) FT-IR spectra of N-CQDs.

domains, which was caused by the oxidation, the increase of structure defects, and attachment of functional groups on the C basal plane [18, 36]. The 2D peak intensity of N-CQDs at about 2,700 cm^{-1} was weakened, and the I_{2G}/I_D intensity ratio was also reduced. This phenomenon illustrated the graphitization of N-CQDs [37], which had more layers than graphene. The detailed information of the functional groups in N-CQDs could be obtained from the FT-IR spectrum shown in Fig. 7(b). The strong and broad peak at 3,332 cm^{-1} was the stretching vibration of –OH, and the peak at 1,620 cm^{-1} represented the flexural vibration of –OH. The peak of C–OH stretching vibration at 1,067 cm^{-1} also indicated the presence of hydroxyl groups. The peak at 1,716 cm^{-1} was the stretching vibration of C=O in carbonyl and carboxyl groups, while the peak at 1,384 cm^{-1} also corresponded to –COOH. Besides, the peaks at 1,259 and 1,245 cm^{-1} showed the existence of C–O–C and C–N in N-CQDs, respectively. Hence, it can be inferred that the synthesized N-CQDs had a structure similar to GO. There were abundant O-containing functional groups including carboxyl (–COOH), hydroxyl (–OH), and epoxy (C–O–C). And the doped N atoms in N-CQDs were mainly distributed as C–N=C, C–NH–C, and N–$(C)_3$. These groups and elemental doping could

change the surface properties of QDs, which played an important role in enhancing their dispersion stability and tribological behavior in nanofluid.

3.2 Tribological behavior of N-CQDs in MoS_2 nanofluid

Figure 8 shows the friction coefficient–time curves as well as the variation of average friction coefficient and wear rate for the base fluid and MoS_2 nanofluids with different N-CQD concentrations. The test load and rotational speed of friction pairs were 300 N and 300 r·min^{-1} (0.377 m·s^{-1}), respectively. It can be seen that the base fluid exhibited a poor lubrication performance that both the friction coefficient and wear rate were the highest. The friction coefficient curve also fluctuated mightily, and the value of friction coefficient increased continuously. When MoS_2 nanoparticles were added to the base fluid, the tribological behavior of lubricants have been improved to some extent. And the addition of N-CQDs further reduced the friction coefficient and wear rate. The optimal concentration of N-CQDs as lubrication additive for MoS_2 nanofluid was 0.4 wt% where the friction coefficient and wear rate were reduced by about 30.4% and 31.0%, respectively, compared to those under MoS_2 lubrication condition. When the concentration of N-CQDs exceeded the optimal concentration of 0.5 wt%, the friction coefficient rebounded slightly, and meanwhile, the increase of wear rate was relatively larger. The reason for this phenomenon was that an excessive concentration will impact the dispersion stability of nanoparticles in nanofluids. Then they were easy to agglomerate, and these large size particles would act as wear particles to deteriorate the tribological behavior of lubricants. Table 2 summarized the tribological properties of the present study and several typical investigations by related scholars. The reduction in friction coefficient after the addition of nanoparticles to base-fluid lubricants was listed. It can be seen that the collaborative use of N-CQDs and MoS_2 in water-based lubricants exhibited strong superiority and competitiveness with other studies in reducing the friction coefficient. Besides, it is worth noting that the curves of lubricants containing nanoparticles were relatively smooth, which reflected the formation of protective tribofilm by complex physical and tribochemical reactions at the friction interface [38].

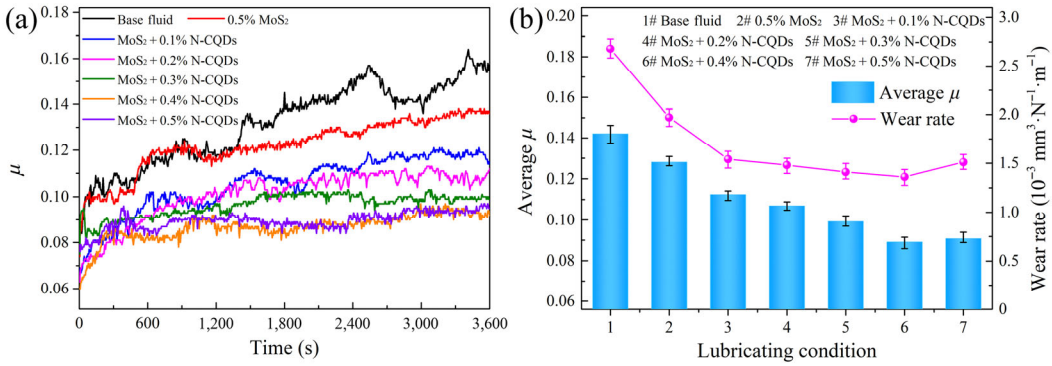

Fig. 8 Pin-on-disk tribological behavior of different lubricants under 300 N and 300 r·min^{-1}: (a) friction coefficient–time curves and (b) average friction coefficient and wear rate.

Table 2 Comparison in the tribological properties of our study and several typical studies.

Nanoparticle	Base fluid	Reduction in μ and corresponding concentration	Test method
Present study	Water-based fluid	37.3% (0.142 to 0.089), 0.4 wt% N-CQDs + 0.5 wt% MoS_2	Pin-on-disk test at 300 N, 300 r·min^{-1}
Hexagonal BN [39]	Water-based fluid	26.3% (0.061 to 0.045), 0.7 wt%	Four-ball test at 392 N, 1,760 r·min^{-1}
Al_2O_3+MoS_2 [40]	O/W emulsion with 5 vol% oils	44.2% (0.278 to 0.155), 1.25 wt%	Turning of AISI 304 steel
WS_2 [41]	Poly-alpha olefin	31.6% (0.114 to 0.078), 0.4 wt%	Four-ball test at 392 N, 1,200 r·min^{-1}
SiO_2–B–N–GO [3]	Base oils	23.9% (0.092 to 0.070), 0.15 wt%	Four-ball test at 392 N, 1,200 r·min^{-1}

And the application of N-CQDs in MoS_2 nanofluid could further promote the generation of stable tribofilm, thus reducing the friction coefficient and wear rate. The detailed mechanism will be discussed in Section 3.5.

The variation of tribological behavior for the nanofluid with MoS_2 + 0.4 wt% N-CQDs with test load was shown in Fig. 9. With the increase of load, the average friction coefficient decreased first and reached the lowest at 200 N, and after that it showed an upward trend. However, the variation of wear rate was complicated, but the wear rate at 500 N was much higher than those at other conditions. And the friction coefficient curve at 500 N exhibited ultra-intense fluctuation, showing that the friction process was unstable. From the results above, several inferences could be drawn. Firstly, within a certain range, the increase of load can contribute to the plastic deformation of the metal surfaces. The asperities on the surfaces will be declined, then friction and wear can be alleviated. Secondly, interfacial tribochemical reactions between nanoparticles and metal surfaces may be more likely to occur under higher pressures, which can also facilitate the formation of tribofilm. Thirdly, when the pressure in the contact area of friction pairs exceeds the bearing capacity of nanofluid, such as 500 N in this study, the lubricant will fail and then cause severe wear. Finally, the related investigation has also confirmed that under relatively higher pressure, nanoparticles are more difficult to enter the friction contact interface to achieve anti-friction and anti-wear effect.

The influence of friction speed on the tribological behavior of nanofluid with MoS_2 + 0.4 wt% N-CQDs at the load of 300 N was explored. As shown in Fig. 10, with the rise of rotational speed from 100 r·min^{-1} (0.126 m·s^{-1}) to 500 r·min^{-1} (0.628 m·s^{-1}), both the friction coefficient and wear rate decreased continuously. The average friction coefficient and wear rate at 500 N were 33.5% and 28.7%, lower than those at 100 N, respectively. According to the classical principle of tribology, the consecutive reduction of friction coefficient with increasing friction speed indicated that the lubrication regime of hybrid nanofluid was

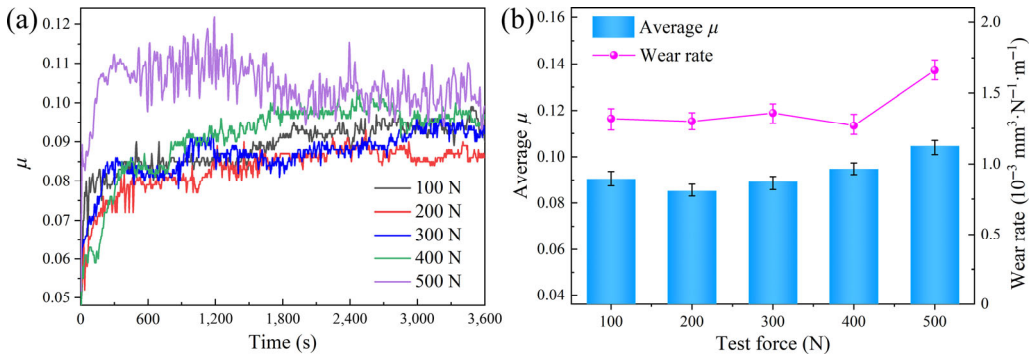

Fig. 9 Variation of (a) friction coefficient–time curves and (b) average friction coefficient and wear rate of MoS_2 + 0.4 wt% N-CQD nanofluid with test load at 300 r·min^{-1}.

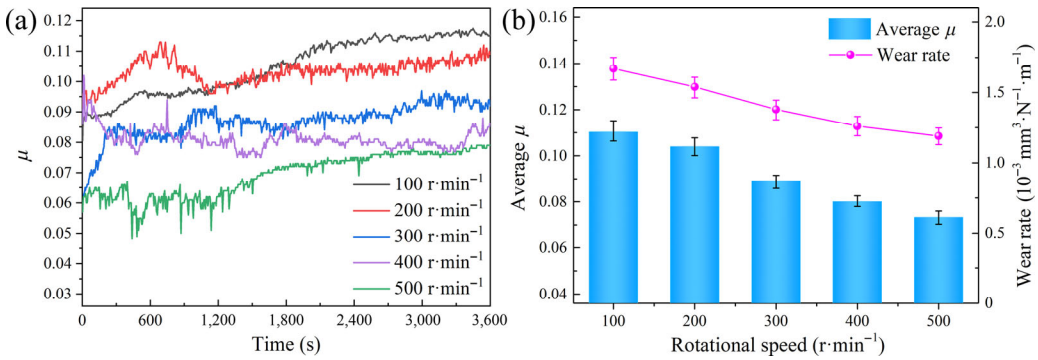

Fig. 10 Variation of (a) friction coefficient–time curves and (b) average friction coefficient and wear rate of MoS_2 + 0.4 wt% N-CQD nanofluid with rotational speed at 300 N.

the mixed lubrication regime, which is a combination of the elasto-hydrodynamic lubrication, boundary lubrication, and thin film lubrication regime [42]. In this condition, the thickness of tribofilm formed by nanofluids on the metal surface will increase with the augment of rotational speed.

3.3 Analysis of the worn surface

The optical images, 3D topographies, and corresponding surface profile curves (along Y = 1,287.0 μm) of the worn disk under different lubrication conditions were characterized and presented in Fig. 11. The test load and rotational speed of steel pin were 300 N and 300 r·min^{-1}, respectively. The average linear roughness (R_a), the maximum peak height (R_p), and the maximum valley depth (R_v) of the profile were also measured. As shown in Fig. 11(a), when the base fluid was applied as lubricant, the wear scar was about 1,577.6 μm in width. Plenty of furrows, asperities, and plastic deformation were observed on the surface, and meanwhile severe adhesive wear occurred as the region marked by the arrow. The grooves reached a maximum depth of nearly 30 μm. As for the worn surface lubricated by MoS_2 nanofluid, the metal adhesion almost disappeared, and the width of wear scar reduced to 1,096.1 μm, but there were still significant grooves and convex peaks caused by abrasive wear. From the profile curves and roughness values, the R_a value of the wear region under MoS_2 nanofluid lubrication condition was basically the same as that lubricated by the base fluid. However, both the R_p and R_v values decreased sharply by about 40.2% and 58.0%, respectively. It can be seen from Fig. 11(c) that when N-CQDs were added to MoS_2 nanofluid, there was no change in the wear form, whereas the wear volume of friction surface was further decreased. The wear scar width was reduced to about 904.3 μm, and meanwhile the surface quality was improved obviously with the lowest roughness values. The furrows became sparse, and the asperities were weakened.

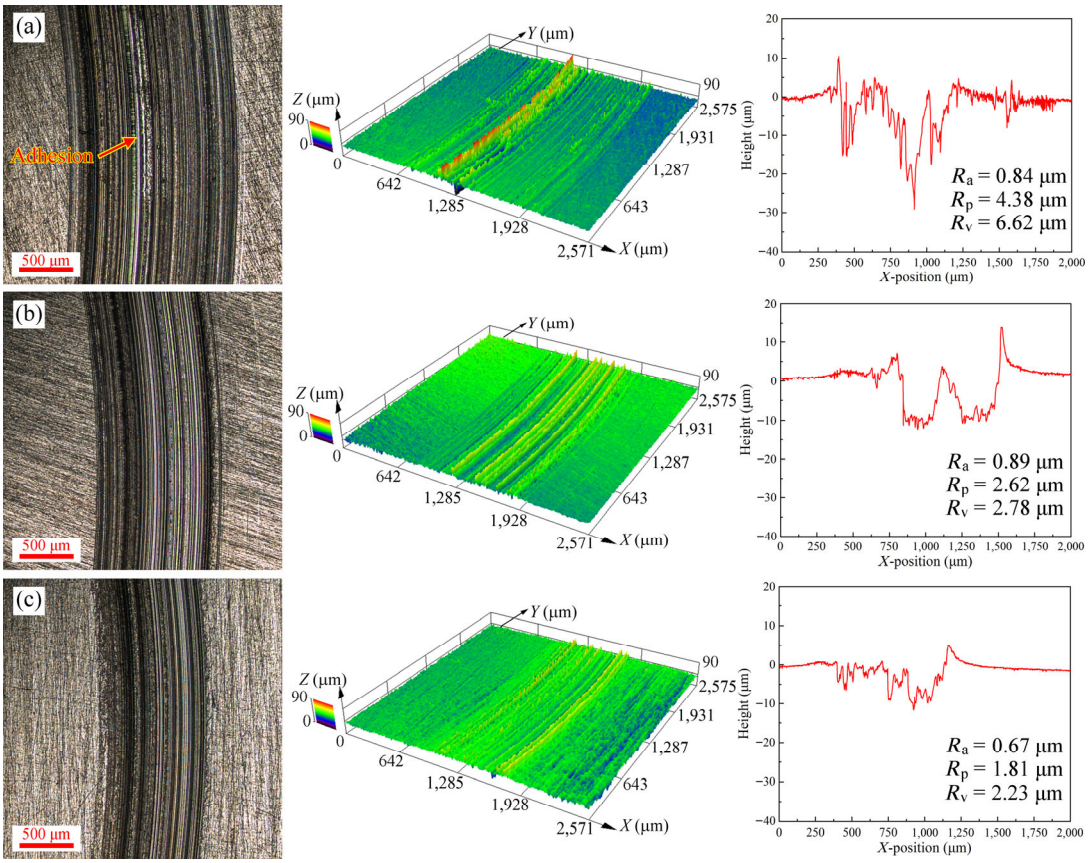

Fig. 11 Optical images, 3D topographies, and profile curves of the worn disk lubricated by (a) base fluid, (b) MoS_2 nanofluid, and (c) MoS_2 + 0.4 wt% N-CQD nanofluid.

Figure 12 shows the SEM images and EDS analysis results of the wear scar on the disk lubricated with MoS_2 and MoS_2 + 0.4 wt% N-CQD nanofluid. As marked in Fig. 12(a), these cracks along the sliding direction in the SEM image for the disk under MoS_2 lubrication condition were attributed to the metal tearing. The wear traces were relatively wide, indicating that the plastic deformation was serious. Nevertheless, the grooves and asperities on the worn surface lubricated by MoS_2 + 0.4 wt% N-CQD nanofluid became relatively finer and shallower. Through the EDS results, it can be found that both C and S elements were distributed evenly on the metal surface, especially in the furrow regions. This phenomenon reflected the mending effect of nanoparticles in lubricant due to their high specific surface area and activity [22]. Then the nanoparticles were easy to deposit and absorb on the metal to repair surface defects [43]. These C elements in the worn surface lubricated by the MoS_2 nanofluid without C-based nanoparticles were derived from the tribo-sintering of dispersants and other organic molecules in the base fluid. Besides, some agglomerated MoS_2 and N-CQD nanoparticles were observed to be attached to the metal surface, which also supported the mending effect illustrated above. The EDS results also shows that the relative content of C and N on the worn surface lubricated by hybrid nanofluid increased, confirming the existence of N-CQDs. In summary, the application of N-CQDs in nanofluids is of great help to achieve a better lubrication performance, thus improving the worn surface quality and reducing material wastage.

3.4 Interfacial tribochemistry and formation of tribofilm

During the friction process, a series of complex physical and chemical processes between the lubricant and metal surface are essential to improve the anti-wear and anti-friction properties. Therefore, the effect of N-CQDs on the tribochemistry at the friction interface and the formation of tribofilm were investigated by means of experiments and MD simulation in this section. Figure 13 shows the XPS results of the worn surface on the disk lubricated by

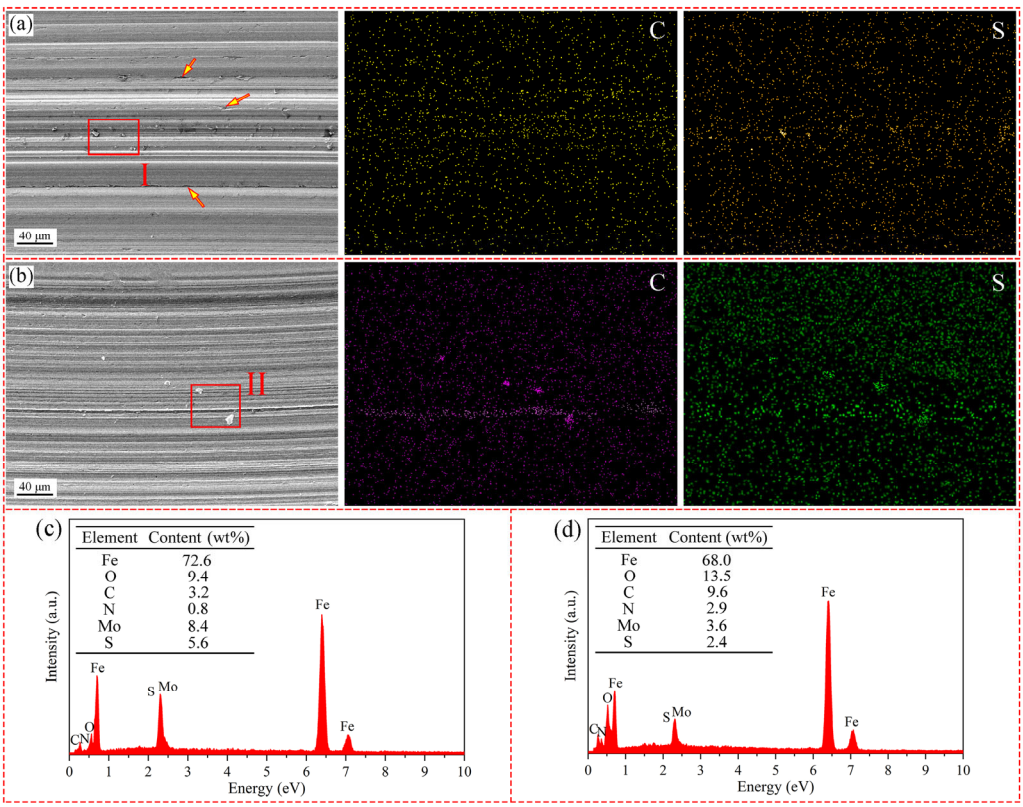

Fig. 12 SEM images and EDS mappings of the worn surfaces on the disk lubricated by (a) MoS_2 nanofluid, (b) MoS_2 + 0.4 wt% N-CQD nanofluid, and the EDS results of (c) Region I and (d) Region II.

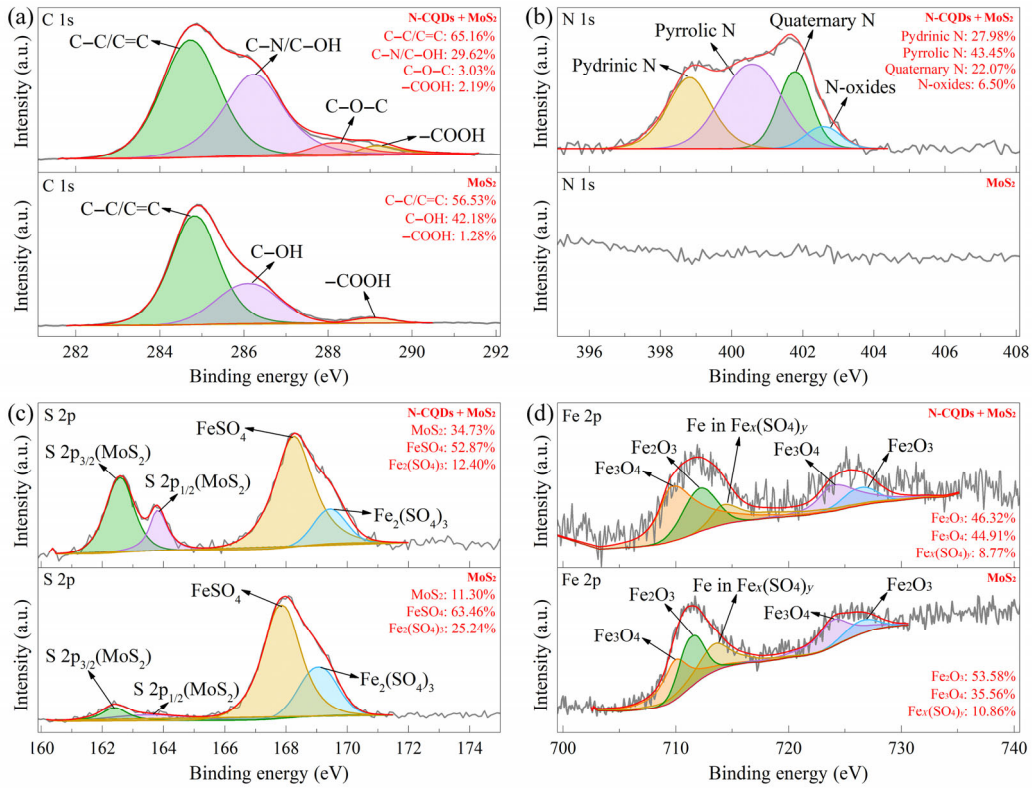

Fig. 13 (a) C 1s, (b) N 1s, (c) S 2p, and (d) Fe 2p XPS spectra of the wear scar on the disk lubricated with MoS_2 and MoS_2 + 0.4 wt% N-CQD nanofluid.

MoS_2 and MoS_2 + 0.4 wt% N-CQD nanofluid to obtain the difference in the chemical states of elements. Firstly, by comparing C 1s spectra between two conditions, it can be found that the peak of C–C/C=C (284.7 eV), C–OH (286.2 eV), and –COOH (289.2 eV) appeared in both, which came from the organic matters and N-CQDs in lubricants. The presence of C–N and C–O–C peak, as well as the increased –COOH content also proved the existence of N-CQDs. The change in the relative content of various groups indicated that the nanoparticles and organic molecules were involved in the continuous breakage and formation of covalent bonds. And related studies have shown that the –OH and –COOH groups were important for the formation of tribofilm [44, 45]. The N 1s peaks in the spectrum of the sample with hybrid nanofluid also confirmed the above inference. It is worth noting that the N 1s peak at 402.6 eV was related to N-oxides. This result showed that due to the high temperature and pressure at friction interface, some of the N-containing groups in N-CQDs were oxidized to $–NO_2$. Consequently, the interaction between nanoparticles and metal surfaces became stronger, which may further reinforce the strength of tribofilm.

As shown in Figs. 13(c) and 13(d), S 2p peaks at 162.6 and 163.8 eV in the spectra were corresponding to MoS_2. Meanwhile, S 2p peaks at 167.9 and 169.1 eV and Fe 2p peak at 713.6 eV could confirm the generation of $FeSO_4$ and $Fe_2(SO_4)_3$. The content of MoS_2 in S-containing substances for the worn surface lubricated with hybrid nanofluid was much lower than that with MoS_2 nanofluid. The Fe $2p_{3/2}$ peaks in the range of 709 to 715 eV and Fe $2p_{1/2}$ peaks in the range of 722 to 729 eV were attributed to iron oxides including Fe_3O_4 and Fe_2O_3. And the proportion of $Fe_x(SO_4)_y$ among all iron-containing substances was basically the same under two lubrication conditions. Hence, it could be deduced that for the surface lubricated with N-CQD/MoS_2 hybrid nanofluid, the decrease in MoS_2 adsorption amount indicated that N-CQDs occupied part of the adsorption sites, similar to the competitive adsorption phenomenon of organic molecules [46]. Besides, the above results showed that with the assistance of local high temperature

and pressure condition of friction processes, MoS_2 nanoparticles have reacted with metal surface in the aqueous environment by Reaction (2):

$$3Fe + 2MoS_2 + 11O_2 = FeSO_4 + Fe_2(SO_4)_3 + 2MoO_3 \quad (2)$$

These newly-formed MoO_3 particles have a similar lamellar structure as MoS_2, which also have the lubrication effect. $FeSO_4$ and $Fe_2(SO_4)_3$ on the worn surface possessed a certain degree of self-lubricating effect [47].

To further confirm the tribochemical process at friction interface illustrated above, the structure and composition of tribofilm were analyzed. As shown in Fig. 14, a tribofilm with the thickness of about 13.9 nm in average was found on the Fe matrix. It can be seen from the HRTEM image in Fig. 14(b) that there were obvious disorderly crystal lattices in the tribofilm region, and the selected area electron diffraction (SAED) pattern presented in Fig. 14(c) showed distinct diffraction rings. Hence, it can be concluded that the film was mainly composed of fine crystal debris and amorphous phase. Our previous research [48] has revealed that there were significant porous areas in the top of the tribofilm formed by nanofluid-containing MoS_2 and Al_2O_3 nanoparticles, but the tribofilm was relatively uniform in this study. This difference indicated that due to the excellent film-forming ability and exfoliation effect [49] of N-CQDs and MoS_2, these nanoparticles were converted into ultra-fine grains through "tribo-sintering" during friction processes. Furthermore, as shown in Fig. 14(d), all these elements were evenly distributed in the tribofilm. The content of S at the interface of Fe matrix and tribofilm was higher than those in other areas, which also reflected the formation of $FeSO_4$ and $Fe_2(SO_4)_3$ on the worn surface.

MD simulation results on the distribution of critical atoms from MoS_2 and N-CQDs between Fe surfaces at the final simulation state (1,000 ps) were shown in Fig. 15. And the corresponding concentration profiles along *z*-direction were also presented. When only MoS_2 nanoparticles were applied, as shown in Fig. 15(a), S atoms tended to be distributed at the interface, while the distribution of Mo atoms was very uniform. Meanwhile, it can be seen from Fig. 15(b) that for the system with N-CQDs and MoS_2, S, N, and O atoms all exhibited the tendency to move toward metal surfaces, but the concentration of S atoms at the interface was lower than that in Fig. 15(a). Besides, the potential energy variations of both systems during simulation process were shown in Fig. S2 in the ESM. The potential energy became stable after about 200 ps. This phenomenon indicated that MD simulation systems have reached a relative equilibrium state that interactions between metal surface and different nanoparticles were stable. This also showed that the MD models and parameters setup in the study were reasonable and scientific. The average values of potential energy in the equilibrium state for

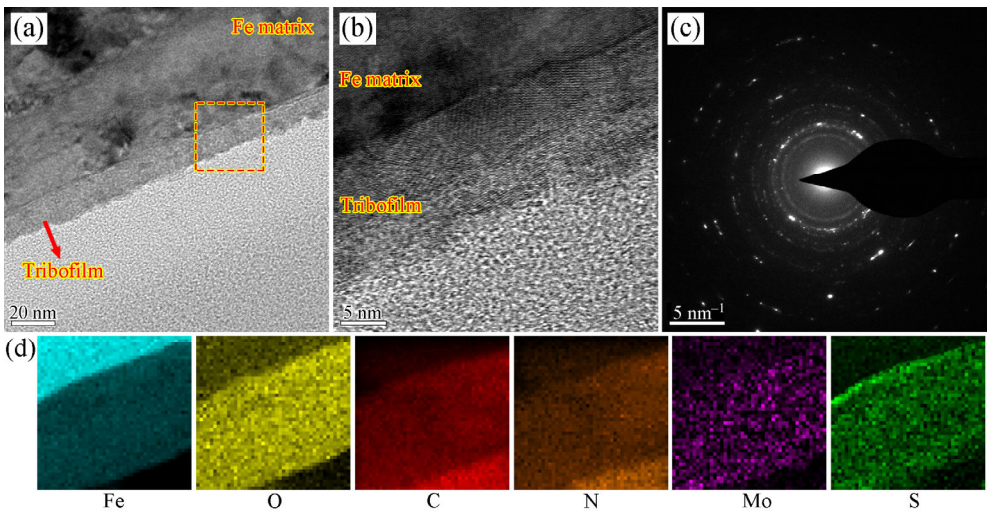

Fig. 14 (a) TEM image, (b) HRTEM image, corresponding (c) SAED pattern, and (d) EDS mapping results of tribofilm formed on the friction surface lubricated with MoS_2 + 0.4 wt% N-CQD nanofluid.

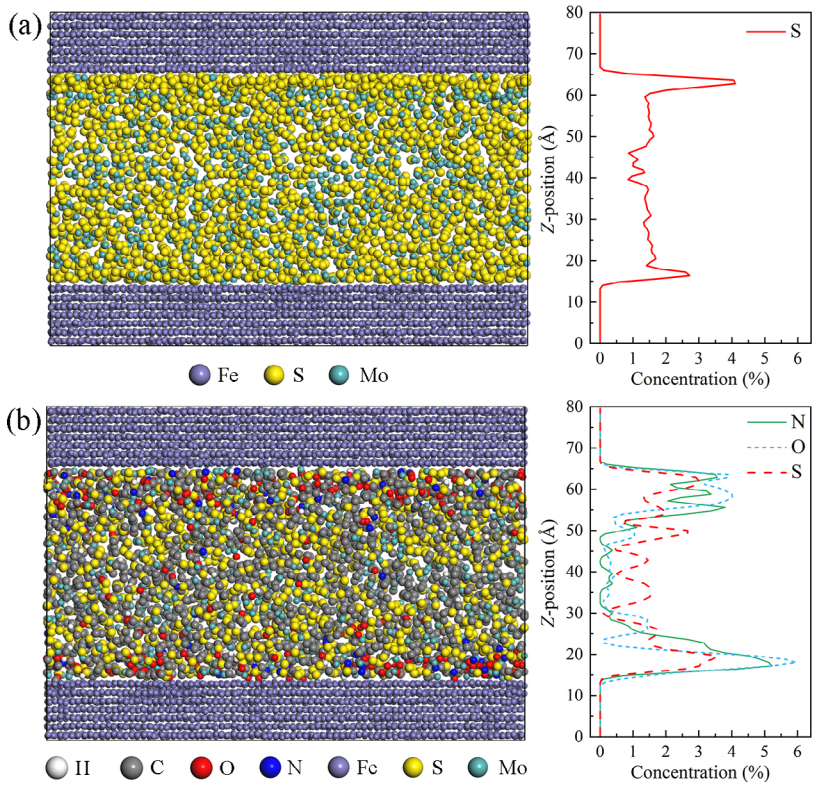

Fig. 15 Distribution and concentration profiles of critical atoms along *z*-direction between friction pairs obtained by MD simulation for the system with (a) MoS_2 and (b) MoS_2 + N-CQD nanoparticles.

MoS_2 and MoS_2 + N-CQD systems were both negative and were −1,834.8 and −2,040.4 kcal·mol^{-1}, respectively. Hence, there was stronger attraction interaction in the system with MoS_2 + N-CQDs than that with MoS_2. It can be inferred that the strength and cohesion of the tribofilm formed by MoS_2 + N-CQD nanofluid were more stable and compact [50], contributing to a better lubrication performance. The diffusion of atoms to surface reflects the adsorption behavior with metal atoms [51], and this plays a vital role in chemical reactions and formation of film at the friction interface. Therefore, it can be determined that the interactions of N-CQDs with metal surface were mainly through various functional groups containing O and N atoms, and for MoS_2 nanoparticles, these effects were primarily achieved by S atoms. Afterwards, other atoms covalently bonded to these active atoms were also attached to the friction surfaces.

3.5 Discussion on the lubrication mechanism of N-CQDs in MoS_2 nanofluid

Based on the above results from experiments and MD simulations, the lubrication mechanism of N-CQDs in MoS_2 nanofluid is proposed and discussed. Firstly, during the friction processes, nanoparticles will move at high speed between metal surfaces. With the high kinetic energy, asperities on the friction surface can be weakened, and then the surface quality is improved by the polishing effect. And this effect can be reinforced when the load increases within a certain range. Secondly, under pressure and shear force, MoS_2 nanoparticles will show the interlayer sliding effect that part of the friction acting on metal surface can be shared out by the internal friction of nanosheets. Meanwhile, the spherical N-CQD nanoparticles may roll between friction surfaces as ball bearings, which converts the sliding friction into rolling friction. Our previous MD study [52] also proved that the joint use of lamellar and spherical nanoparticles could exhibit a synergistic lubrication performance to alleviate friction and wear. Similarly, from the aspect of motion mode of nanoparticles, the S atoms of MoS_2 nanoparticles in this study could transfer and absorb on N-CQD surface to promote the rolling motion.

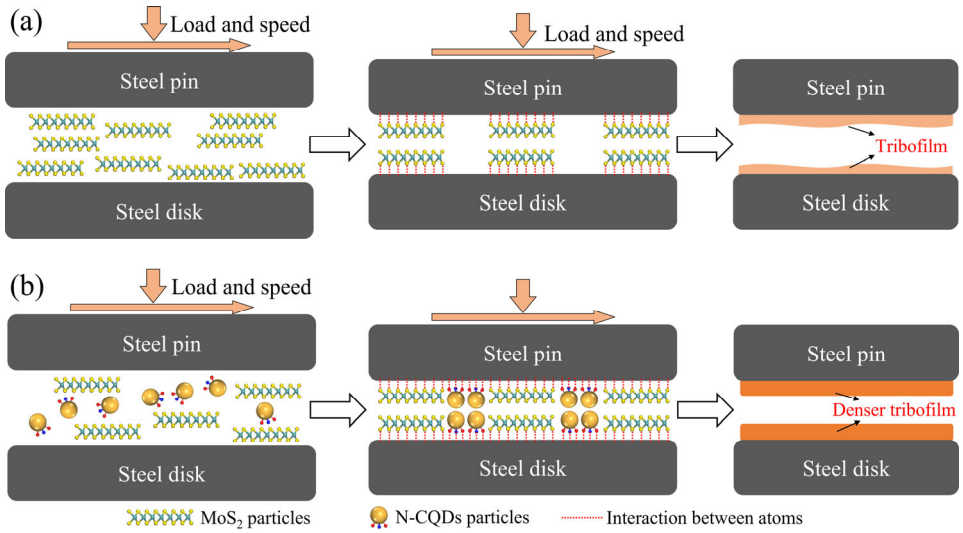

Fig. 16 Formation of tribofilm on the friction surface lubricated with (a) MoS_2 and (b) MoS_2 + N-CQD nanofluid.

And the rolling motion also in turn enhanced the interlayer sliding effect of MoS_2 nanosheets. From the aspect of their physicochemical properties, the spherical N-CQD nanoparticles could separate different MoS_2 monolayers, weakening their chemical reactions, entanglement, and other phenomena that may inhibit the interlayer sliding effect. At the same time, MoS_2 nanosheets could prevent the hard N-CQD nanoparticles from embedding into Fe matrix, which ensured the natural rolling motion of N-CQD particles and also reduced the wear on friction surface. These effects contributed to the better lubrication performance of nanofluid synergistically. Thirdly, as shown in Fig. 16, induced by the tribochemistry at friction interface, nanoparticles and organic molecules in the nanofluid will deposit and adsorb on the metal surface. Then a series of reactions will appear, and the friction surface will be covered by a protective tribofilm. Several nanoparticles break up and exfoliate into smaller crystal particles, afterwards MoS_2 particles can attach to the metal surface by their S atoms. The O atoms in O-containing groups (–OH, –COOH, and C–O–C) and N atoms in N-containing groups (C–N and $–NO_2$) of N-CQDs can form attraction with Fe atoms through hydrogen bonding and van der Waals interaction, which enhances the absorption intensity of N-CQDs with metal surface. Besides, according to the investigation by Ye et al. [53], abundant positive charges will generate on the metal surface, thereby the absorption of these O- and N-containing functional groups will be rapider and easier. As a result, due to the stronger adsorption capacity of N-CQDs than that of MoS_2 nanoparticles, the tribofilm formed by MoS_2/N-CQD hybrid nanofluid may be more compact and firmer than that by MoS_2 nanofluid. Hence, the addition of N-CQDs to nanofluid can improve the lubrication performance. The tribofilm can avoid the direct contact of friction pairs effectively, which is important to protect the metal surface from serious wear. And the nanostructured crystal particles, multicomponent amorphous substances, as well as the tribochemistry-induced $FeSO_4/Fe_2(SO_4)_3$ have self-lubricating effect, contributing to friction and wear mitigation at the interface.

4 Conclusions

The present research provided a novel method to synthesize N-CQD nanoparticles, which significantly enhanced the tribological behaviors of MoS_2 nanofluid. The related tribochemistry-induced lubrication mechanism was revealed through experiments and MD simulation. The characterization of N-CQD particles indicated that they exhibited a GO-like structure containing abundant O- and N-containing functional groups. Adding 0.4 wt% N-CQDs into MoS_2 nanofluid could achieve the optimal lubrication performance that contributed to approximately 30.4% and 31.0% reduction in the friction coefficient and wear rate with the mixed lubrication regime.

Nanoparticles were found to be deposited and absorbed on the worn surface lubricated with MoS_2 + N-CQD nanofluid. A defensive tribofilm with the average thickness of ~13.9 nm was generated at the friction interface, which was composed of amorphous substances, ultrafine crystalline N-CQD/MoS_2 particles, and self-lubricating $FeSO_4$/$Fe_2(SO_4)_3$. Combined with the MD simulation results, the interaction between S atoms in MoS_2 and various functional groups in N-CQDs (mainly –OH, –COOH, C–O–C, C–N, and –NO_2) with metal surfaces promoted the deposition and tribochemical reactions of nanoparticles. This further improved the stability and compactness of the tribofilm, and then the metal surface could be better protected from severe wear. All these results proved that the novel eco-friendly N-CQDs with superior would be a potential lubricant additive in industrial applications. And this study could also provide a reference for related investigations in the future.

Acknowledgements

This work was supported by the National Natural Science Foundation of China (No. 51874036) and Beijing Municipal Natural Science Foundation (No. 2182041).

Electronic Supplementary Material Supplementary material is available in the online version of this article at https://doi.org/10.1007/s40544-022-0619-4.

References

[1] Xiong S, Liang D, Wu H, Lin W, Chen J S, Zhang B S. Preparation, characterization, tribological and lubrication performances of Eu doped $CaWO_4$ nanoparticle as anti-wear additive in water-soluble fluid for steel strip during hot rolling. *Appl Surf Sci* **539**: 148090 (2021)

[2] Ishikawa T, Choi J. Effect of water adsorption on the frictional properties of hydrogenated amorphous carbon films in various relative humidities. *Langmuir* **37**(3): 1012–1024 (2021)

[3] Xiong S, Zhang B S, Luo S, Wu H, Zhang Z. Preparation, characterization, and tribological properties of silica-nanoparticle-reinforced B–N-co-doped reduced graphene oxide as a multifunctional additive for enhanced lubrication. *Friction* **9**(2): 239–249 (2021)

[4] Huang P, Qi W, Yin X, Choi J, Chen X C, Tian J S, Xu J X, Wu H C, Luo J B. Ultra-low friction of a-C:H films enabled by lubrication of nanodiamond and graphene in ambient air. *Carbon* **154**: 203–210 (2019)

[5] Yan Z Y, Chen J, Xiao A, Shu J, Chen J Q. Effects of representative quantum dots on microorganisms and phytoplankton: A comparative study. *RSC Adv* **5**(129): 106406–106412 (2015)

[6] Dutta S, Chatterjee S, Mallem K, Cho Y H, Yi J. Control of size and distribution of silicon quantum dots in silicon dielectrics for solar cell application: A review. *Renew Energy* **144**: 2–14 (2019)

[7] Huang H, Hu H L, Qiao S, Bai L, Han M M, Liu Y, Kang Z H. Carbon quantum dot/CuS_x nanocomposites towards highly efficient lubrication and metal wear repair. *Nanoscale* **7**(26): 11321–11327 (2015)

[8] Tang W W, Zhang Z, Li Y F. Applications of carbon quantum dots in lubricant additives: A review. *J Mater Sci* **56**(21): 12061–12092 (2021)

[9] Tang J Z, Chen S Q, Jia Y L, Ma Y, Xie H M, Quan X, Ding Q. Carbon dots as an additive for improving performance in water-based lubricants for amorphous carbon (a-C) coatings. *Carbon* **156**: 272–281 (2020)

[10] Xiao H P, Liu S H, Xu Q, Zhang H. Carbon quantum dots: An innovative additive for water lubrication. *Sci China Technol Sci* **62**(4): 587–596 (2019)

[11] Alam A M, Park B Y, Ghouri Z K, Park M, Kim H Y. Synthesis of carbon quantum dots from cabbage with down- and up-conversion photoluminescence properties: Excellent imaging agent for biomedical applications. *Green Chem* **17**(7): 3791–3797 (2015)

[12] Das R, Bandyopadhyay R, Pramanik P. Carbon quantum dots from natural resource: A review. *Mater Today Chem* **8**: 96–109 (2018)

[13] Tu Z Q, Hu E Z, Wang B B, David K D, Seeger P, Moneke M, Stengler R, Hu K H, Hu X G. Tribological behaviors of Ni-modified citric acid carbon quantum dot particles as a green additive in polyethylene glycol. *Friction* **8**(1): 182–197 (2020)

[14] Sarno M, Abdalglil Mustafa W A, Senatore A, Scarpa D. One-step "green" synthesis of dispersable carbon quantum dots/poly(methyl methacrylate) nanocomposites for tribological applications. *Tribol Int* **148**: 106311 (2020)

[15] Mou Z H, Zhao B, Wang B G, Xiao D. Integration of functionalized polyelectrolytes onto carbon dots for synergistically improving the tribological properties of polyethylene glycol. *ACS Appl Mater Interfaces* **13**(7): 8794–8807 (2021)

[16] He J Q, Sun J L, Meng Y N, Pei Y. Superior lubrication performance of MoS_2–Al_2O_3 composite nanofluid in strips hot rolling. *J Manuf Process* **57**: 312–323 (2020)

[17] Ali M K A, Hou X J, Abdelkareem M A A. Anti-wear properties evaluation of frictional sliding interfaces in automobile engines lubricated by copper/graphene nanolubricants. *Friction* **8**(5): 905–916 (2020)

[18] Du S N, Sun J L, Wu P. Preparation, characterization and lubrication performances of graphene oxide–TiO_2 nanofluid in rolling strips. *Carbon* **140**: 338–351 (2018)

[19] Zheng X J, Xu Y F, Geng J, Peng Y B, Olson D, Hu X G. Tribological behavior of Fe_3O_4/MoS_2 nanocomposites additives in aqueous and oil phase media. *Tribol Int* **102**: 79–87 (2016)

[20] Saleem M, Naz M Y, Shukrullah S, Shujah M A, Akhtar M, Ullah S, Ali S. One-pot sonochemical preparation of carbon dots, influence of process parameters and potential applications: A review. *Carbon Lett* **32**: 39–55 (2022)

[21] Wu H, Zhao J W, Xia W Z, Cheng X W, He A S, Yun J H, Wang L Z, Huang H, Jiao S H, Huang L, et al. A study of the tribological behaviour of TiO_2 nano-additive water-based lubricants. *Tribol Int* **109**: 398–408 (2017)

[22] Wang B B, Zhong Z D, Qiu H, Chen D X, Li W, Li S J, Tu X H. Nano serpentine powders as lubricant additive: Tribological behaviors and self-repairing performance on worn surface. *Nanomaterials* **10**(5): 922 (2020)

[23] Reinert L, Schütz S, Suárez S, Mücklich F. Influence of surface roughness on the lubrication effect of carbon nanoparticle-coated steel surfaces. *Tribol Lett* **66**: 45 (2018)

[24] Cho D H, Kim J S, Kwon S H, Lee C, Lee Y Z. Evaluation of hexagonal boron nitride nano-sheets as a lubricant additive in water. *Wear* **302**(1–2): 981–986 (2013)

[25] Wang C L, Sun J L, Wu P, Ge C L, Meng W X. Microstructural characterization and tribological behavior analysis on triethanolamine functionalized reduced graphene oxide. *Surf Topogr Metrol Prop* **9**(2): 025023 (2021)

[26] Chou C C, Lee S H. Tribological behavior of nanodiamond-dispersed lubricants on carbon steels and aluminum alloy. *Wear* **269**(11–12): 757–762 (2010)

[27] Sneha E, Revikumar A, Singh J Y, Thampi A D, Rani S. Viscosity prediction of Pongamia pinnata (Karanja) oil by molecular dynamics simulation using GAFF and OPLS force field. *J Mol Graph Model* **101**: 107764 (2020)

[28] Konishi M, Washizu H. Understanding the effect of the base oil on the physical adsorption process of organic additives using molecular dynamics. *Tribol Int* **149**: 105568 (2020)

[29] Shi J Q, Fang L, Sun K. Friction and wear reduction via tuning nanoparticle shape under low humidity conditions: A nonequilibrium molecular dynamics simulation. *Comp Mater Sci* **154**: 499–507 (2018)

[30] Brady J F, Bossis G. The rheology of concentrated suspensions of spheres in simple shear flow by numerical simulation. *J Fluid Mech* **155**: 105–129 (1985)

[31] Ewen J P, Heyes D M, Dini D. Advances in nonequilibrium molecular dynamics simulations of lubricants and additives. *Friction* **6**(4): 349–386 (2018)

[32] Lin E Q, Niu L S, Shi H J, Duan Z. Molecular dynamics simulation of nano-scale interfacial friction characteristic for different tribopair systems. *Appl Surf Sci* **258**(6): 2022–2028 (2012)

[33] Burrows S A, Korotkin I, Smoukov S K, Boek E, Karabasov S. Benchmarking of molecular dynamics force fields for solid–liquid and solid–solid phase transitions in alkanes. *J Phys Chem B* **125**(19): 5145–5159 (2021)

[34] Evans D J, Holian B L. The Nose–Hoover thermostat. *J Chem Phys* **83**(8): 4069–4074 (1985)

[35] Fu J, Wei C, Wang W, Wei J L, Lv J. Studies of structure and properties of graphene oxide prepared by ball milling. *Mater Res Innov* **19**(S1): S1-277–S1-280 (2015)

[36] Ray S C, Saha A, Basiruddin S K, Roy S S, Jana N R. Polyacrylate-coated graphene-oxide and graphene solution via chemical route for various biological application. *Diam Relat Mater* **20**(3): 449–453 (2011)

[37] Muzyka R, Drewniak S, Pustelny T, Chrubasik M, Gryglewicz G. Characterization of graphite oxide and reduced graphene oxide obtained from different graphite precursors and oxidized by different methods using Raman spectroscopy. *Materials* **11**(7): 1050 (2018)

[38] Tang H J, Sun J L, He J Q, Wu P. Research progress of interface conditions and tribological reactions: A review. *J Ind Eng Chem* **94**: 105–121 (2021)

[39] He J Q, Sun J L, Meng Y N, Yan X D. Preliminary investigations on the tribological performance of hexagonal boron nitride nanofluids as lubricant for steel/steel friction pairs. *Surf Topogr*: *Metrol Prop* **7**(1): 015022 (2019)

[40] Sharma A K, Singh R K, Dixit A R, Tiwari A K. Novel uses of alumina–MoS_2 hybrid nanoparticle enriched cutting fluid in hard turning of AISI 304 steel. *J Manuf Process* **30**: 467–482 (2017)

[41] Jiang Z Q, Zhang Y J, Yang G B, Gao C P, Yu L G, Zhang S M, Zhang P Y. Synthesis of oil-soluble WS_2 nanosheets under mild condition and study of their effect on tribological properties of poly-alpha olefin under evaluated temperatures. *Tribol Int* **138**: 68–78 (2019)

[42] Wen S Z, Huang P, Tian Y, Ma L R. *Principle of Tribology*, 5th edn. Beijing (China): Tsinghua University Press, 2018.

[43] Thrush S J, Comfort A S, Dusenbury J S, Xiong Y Z, Qu H W, Han X, Schall J D, Barber G C, Wang X. Stability, thermal conductivity, viscosity, and tribological characterization of zirconia nanofluids as a function of nanoparticle concentration. *Tribol Trans* **63**(1): 68–76 (2020)

[44] Matsui Y, Aoki S, Masuko M. Elucidation of the action of functional groups in the coexisting ashless compounds on the tribofilm formation and friction characteristic of zinc dialkyldithiophosphate-formulated lubricating oils. *Tribol Trans* **61**(2): 220–228 (2018)

[45] Padenko E, van Rooyen L J, Wetzel B, Karger-Kocsis J. "Ultralow" sliding wear polytetrafluoro ethylene nano-composites with functionalized graphene. *J Reinf Plast Compos* **35**(11): 892–901 (2016)

[46] Ngo D, He X, Luo H M, Qu J, Kim S H. Competitive adsorption of lubricant base oil and ionic liquid additives at air/liquid and solid/liquid interfaces. *Langmuir* **36**(26): 7582–7592 (2020)

[47] Xiong S, Sun J L, Xu Y, Yan X D, Li Y. Tribological performance and wear mechanism of compound containing S, P, and B as EP/AW additives in copper foil oil. *Tribol Trans* **59**(3): 421–427 (2016)

[48] He J Q, Sun J L, Meng Y N, Tang H J, Wu P. Improved lubrication performance of MoS_2–Al_2O_3 nanofluid through interfacial tribochemistry. *Colloids Surf A Physicochem Eng Aspects* **618**: 126428 (2021)

[49] Liu Y, Zhang X F, Dong S L, Ye Z Y, Wei Y D. Synthesis and tribological property of $Ti_3C_2T_x$ nanosheets. *J Mater Sci* **52**(4): 2200–2209 (2017)

[50] Pebdani M H, Miller R E. Molecular dynamics simulation of pull-out halloysite nanotube from polyurethane matrix. *Adv Mech Eng* **13**(9) (2021) https://doi.org/10.1177/16878140211044663

[51] Blanck S, Loehlé S, Steinmann S N, Michel C. Adhesion of lubricant on aluminium through adsorption of additive head-groups on γ-alumina: A DFT study. *Tribol Int* **145**: 106140 (2020)

[52] He J Q, Sun J L, Meng Y N, Pei Y, Wu P. Synergistic lubrication effect of Al_2O_3 and MoS_2 nanoparticles confined between iron surfaces: A molecular dynamics study. *J Mater Sci* **56**(15): 9227–9241 (2021)

[53] Ye M T, Cai T, Shang W J, Zhao L N, Zhang Y X, Liu D, Liu S G. Friction-induced transfer of carbon quantum dots on the interface: Microscopic and spectroscopic studies on the role of inorganic–organic hybrid nanoparticles as multifunctional additive for enhanced lubrication. *Tribol Int* **127**: 557–567 (2018)

Jiaqi HE. He received his bachelor degree in 2017 from China University of Petroleum (East China), China. Now he is a Ph.D. student in University of Science and Technology Beijing, China. His research interests include metal-working lubrication, preparation of nanofluids, and molecular dynamics simulations.

Jianlin SUN. He received his bachelor degree in 1985 from the National Defense University of Technology, China and received Ph.D. degree in 1998 from the Central South University of Technology, China. Now he is a professor of University of Science and Technology Beijing, China. He specializes in friction, wear and lubrication, as well as surface quality control during metal-forming, quantum chemical calculation, and molecular dynamics simulations.

Junho CHOI. He received his bachelor degree in 1994 and master degree in 1996 from Korea University, Republic of Korea. He obtained his Ph.D. degree from The University of Tokyo, Japan, in 2000. Since 2010, he has been an associate professor in the Department of Mechanical Engineering, The University of Tokyo, Japan. His research interests are surface engineering and tribology, including plasma coating, triboelectric nanogenerator, diamond-like carbon films, nano-carbon materials and so on.

Chenglong WANG. He received his master degree in 2019 from University of Science and Technology Beijing, China. He is now a Ph.D. student in University of Science and Technology Beijing. His research focuses on metal working, friction and wear, and nano-lubrication.

Daoxin SU. He received his bachelor degree in 2019 from Hohai University, China. Now he is a postgraduate student in University of Science and Technology Beijing, China. His research interests are surface quality control and lubrication during metal-forming.